

## Density profile of ambient circumnuclear medium in Seyfert 1 galaxies

YIJUN WANG (王倚君)<sup>1,2,3,4</sup> ZHICHENG HE (何志成)<sup>3,4</sup> JUNJIE MAO (毛俊捷)<sup>5,6</sup> JELLE KAASTRA<sup>6,7</sup>  
YONGQUAN XUE (薛永泉)<sup>3,4</sup> AND MISSAGH MEHDIPOUR<sup>8</sup>

<sup>1</sup>*Department of Astronomy, Nanjing University, Nanjing 210093, China*

<sup>2</sup>*Key Laboratory of Modern Astronomy and Astrophysics (Nanjing University), Ministry of Education, Nanjing 210093, China*

<sup>3</sup>*CAS Key Laboratory for Research in Galaxies and Cosmology, Department of Astronomy, University of Science and Technology of China, Hefei 230026, China*

<sup>4</sup>*School of Astronomy and Space Science, University of Science and Technology of China, Hefei 230026, China*

<sup>5</sup>*Department of Physical, Hiroshima University, 1-3-1 Kagamiyama, HigashiHiroshima, Hiroshima 739-8526, Japan*

<sup>6</sup>*SRON Netherlands Institute for Space Research, Niels Bohrweg 4, 2333 CA Leiden, The Netherlands*

<sup>7</sup>*Leiden Observatory, Leiden University, Niels Bohrweg 2, 2300 RA Leiden, The Netherlands*

<sup>8</sup>*Space Telescope Science Institute, 3700 San Martin Drive, Baltimore, MD 21218, USA*

### ABSTRACT

The shape of the ambient circumnuclear medium (ACM) density profile can probe the history of accretion onto the central supermassive black hole in galaxies and the circumnuclear environment. However, due to the limitation of the instrument resolution, the density profiles of the ACM for most of galaxies remain largely unknown. In this work, we propose a novel method to measure the ACM density profile of active galactic nucleus (AGN) by the equilibrium between the radiation pressure on the warm absorbers (WAs, a type of AGN outflows) and the drag pressure from the ACM. We study the correlation between the outflow velocity and ionization parameter of WAs in each of the five Seyfert 1 galaxies (NGC 3227, NGC 3783, NGC 4051, NGC 4593, and NGC 5548), inferring that the density profile of the ACM is between  $n \propto r^{-1.7}$  and  $n \propto r^{-2.15}$  ( $n$  is number density and  $r$  is distance) from 0.01 pc to pc scales in these five AGNs. Our results indicate that the ACM density profile in Seyfert 1 galaxies is steeper than the prediction by the spherically symmetric Bondi accretion model and the simulated results of the hot accretion flow, but more in line with the prediction by the standard thin disk model.

*Keywords:* Galaxies: Seyfert (1447) — Galaxies: nuclei (609) — Galaxies: ISM (847) — X-rays: galaxies (1822) — Accretion, accretion disks (562)

### 1. INTRODUCTION

The ambient circumnuclear medium (ACM) in the center of galaxies can probe the accretion history of the central supermassive black hole (SMBH) in galaxies. Different accretion models correspond to different density profiles of the ACM. The classical Bondi accretion (spherically symmetrical accretion; Bondi 1952) predicts that the density profile of the accretion flow is  $n \propto r^{-1.5}$  ( $n$  is number density and  $r$  is distance) within the Bondi radius, and is a constant at larger radii (Frank et al. 2002). The density profile of the hot accretion flow,

such as advection-dominated accretion flows (ADAFs; Narayan & Yi 1994; Yuan & Narayan 2014, for a review), is between  $n \propto r^{-0.5}$  and  $n \propto r^{-1}$  according to simulations (Yuan et al. 2012). The theory of the standard cold, thin accretion disk (Shakura & Sunyaev 1973) predicts that the density profile of the accretion flow is  $n \propto r^{-15/8}$  (Frank et al. 2002). The multi-wavelength observations toward the center of the Milky Way (MW) indicated that the density profile of the ACM is  $n \propto r^{-1}$  at several hundred Schwarzschild radii (Gillessen et al. 2019), and  $n \propto r^{-1.5}$  in the hot gas halo at the kpc scale (Miller & Bregman 2015). *Chandra* X-ray observations toward the center of M87 and NGC 3115 show that the density profiles of their ACM are  $n \propto r^{-1}$  within the Bondi radius (Russell et al. 2015; Wong et al. 2011). However, due to the limitation of the instrument resolu-

tion, the density profiles of the ACM for most galaxies are still unknown. One way to infer the density profile of the ACM is through fitting the spectral energy distribution of tidal disruption events (TDEs; a star disrupted by the tidal forces from the SMBH), which can trace the interaction process between the outflows from TDEs and the ACM (Alexander et al. 2016; Eftekhari et al. 2018; Anderson et al. 2020; Alexander et al. 2020). However, TDEs are only detected in a small number of galaxies and are difficult to be identified in active galactic nuclei (AGNs) (Gezari 2021). Besides, for AGNs, the emission from the accretion disk or jet will overshadow the emission from the interaction between outflows and ACM at small scales. In this work, we propose a novel way to estimate the density profile of the ACM in AGNs.

AGNs usually play an important role in forming and driving outflows which might further affect the star formation of their host galaxies (He et al. 2019; Chen et al. 2022; King & Pounds 2015, for a review). These outflows might interact with the ACM. Warm absorbers (WAs) are part of AGN ionized outflows (e.g., Laha et al. 2014), which are detected in roughly half of nearby AGNs (e.g., Reynolds 1997; Kaastra et al. 2000; Tombesi et al. 2013). WAs usually consist of several ionization phases (e.g., Laha et al. 2014) and are located from the accretion disk to the narrow-line region (e.g., Reynolds & Fabian 1995; Elvis 2000; Blustin et al. 2005). WAs have the outflowing velocities up to a few thousand of  $\text{km s}^{-1}$  (e.g., Kaastra et al. 2000; Ebrero et al. 2013), and are considered to be driven by radiation pressure (e.g., Proga & Kallman 2004), magnetic forces (e.g., Blandford & Payne 1982; Fukumura et al. 2010), or thermal pressure (e.g., Begelman et al. 1983; Mizumoto et al. 2019).

For the radiatively driven outflowing mechanism, the outflow momentum rate  $\dot{P}_{\text{out}} (\propto n_{\text{H}} r^2 v_{\text{out}}^2)$  approximates to the momentum flux of the radiation field  $\dot{P}_{\text{rad}} (\equiv L_{\text{bol}}/c)$  (Gofford et al. 2015), which can produce a simple scaling relation of  $v_{\text{out}} \propto \xi^{0.5}$  (Tombesi et al. 2013). For the magneto-hydrodynamically (MHD) driven outflowing mechanism, Fukumura et al. (2010) suggested a few scaling relations between  $v_{\text{out}}$ ,  $r$ , and  $\xi$ :  $v_{\text{out}} \propto r^{-\frac{1}{2}} \propto \xi^{\frac{1}{2(2q-1)}}$ . Behar (2009) indicated that the parameter  $q$  is between  $\frac{6}{7}$  and 1 for WA outflowing winds in Seyfert galaxies. Therefore, the scaling relation between  $v_{\text{out}}$  and  $\xi$  in the MHD scenario is estimated to be between  $v_{\text{out}} \propto \xi^{0.5}$  and  $v_{\text{out}} \propto \xi^{0.7}$  (see Figure 1). However, the observational results show that the index of  $v_{\text{out}}-\xi$  relation is usually smaller than 0.5 (e.g., Tombesi et al. 2013; Laha et al. 2014) or see Figure 1 in this work, which cannot be explained by the above models.

**Table 1.** Basic properties of each object for the six Seyfert galaxies and previously published X-ray data used in this work.

Source	Seyfert type	Redshift	WA references
NGC 3227	Sy1.5	0.004	Wang et al. (2022) <sup>1</sup>
NGC 3783	Sy1	0.010	Fu et al. (2017) <sup>1</sup> Mao et al. (2019) <sup>1,2</sup>
NGC 4051	Sy1.5	0.002	Lobban et al. (2011) <sup>2</sup>
NGC 4593	Sy1	0.008	Ebrero et al. (2013) <sup>1,2</sup>
NGC 5548	Sy1.5	0.017	Ebrero et al. (2016) <sup>1,2</sup>
NGC 7469	Sy1.2	0.016	Mehdipour et al. (2018) <sup>2</sup>

NOTE—Seyfert type and redshift of each object are obtained from the NASA/IPAC Extragalactic Database (NED). X-ray data: <sup>1</sup>XMM-Newton; <sup>2</sup>Chandra.

In this work, we consider that WAs are in a pressure equilibrium state, which means that the radiation pressure on the WAs is comparable to the drag pressure from the ACM. With that, we will use the fitting results for the  $v_{\text{out}} - \xi$  relation of WAs to infer the shape of the density profile of the ACM in AGNs. The structure of this work is shown as follows. The method that is applied to infer the density profile of the ACM in AGNs is described in Section 2. In Section 3, we introduce the historical data that are used in this work. In Section 4, we show the fitting results of the observational data, which are further used to infer the density profile of the ACM in AGNs. In Section 5, we discuss the scope of application of our method. Finally, we summarize our conclusions in Section 6.

## 2. METHOD

The outflows in AGN might be driven by multiple mechanisms, for simplicity, we only consider the radiatively driven outflowing mechanism in this work. The radiation pressure from the AGN radiation on the WA gas (Mo et al. 2010) is

$$P_{\text{rad}} = \frac{L_{\text{ion}}}{4\pi r^2 c}, \quad (1)$$

where  $L_{\text{ion}}$  is the ionizing luminosity over 1–1000 Ryd,  $r$  is the radial distance of the absorbing gas to the central engine, and  $c$  is the speed of light. The drag pressure (Batchelor 2000) produced by the ACM on the WAs is

$$P_{\text{D}} = \frac{1}{2} C_{\text{D}} n_{\text{ACM}} m_{\text{p}} v_{\text{out}}^2, \quad (2)$$

where  $C_{\text{D}}$  is the drag coefficient which is probably equal to 1 for compressible gas or clouds,  $n_{\text{ACM}}$  is the number

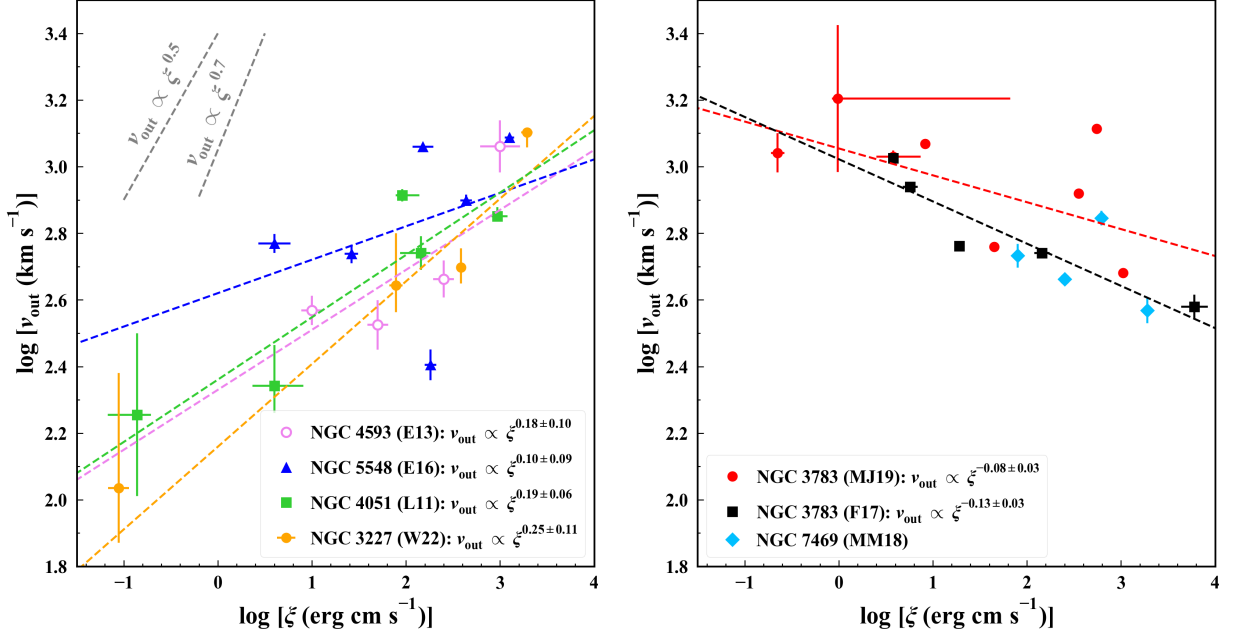


**Figure 1.** The correlation between the outflow velocity ( $v_{\text{out}}$ ) and ionization parameter ( $\xi$ ) for the following six Seyfert 1 galaxies: NGC 3227 (orange solid circles in the left panel), NGC 3783 (red solid circles and black squares in the right panel), NGC 4051 (green squares in the left panel), NGC 4593 (pink hollow circles in the left panel), NGC 5548 (blue triangles in the left panel), and NGC 7469 (sky-blue diamonds in the right panel). The observational data are from the previously published papers: Wang et al. (2022) (W22), Fu et al. (2017) (F17), Mao et al. (2019) (MJ19), Lobban et al. (2011) (L11), Ebrero et al. (2013) (E13), Ebrero et al. (2016) (E16), and Mehdipour et al. (2018) (MM18). The dashed lines represent the best-fit linear models. The best-fit linear model for NGC 7469 cannot be constrained (see Table 2), so only the observational data are shown here. The gray dashed lines in the top left corner of the left panel represent the predicted correlations of radiation-driven and MHD-driven outflowing mechanisms.

density of the ACM, and  $m_p$  is the proton mass. The outflowing velocities of WAs are nearly constant during several years (e.g., Silva et al. 2018). In this work we assume that WAs are in a pressure equilibrium state where the radiation pressure on the WAs is comparable to the drag pressure from the ACM:

$$P_{\text{rad}} \simeq P_D. \quad (3)$$

According to Tarter et al. (1969), the ionization parameter of WAs can be defined by

$$\xi = \frac{L_{\text{ion}}}{n_e r^2}, \quad (4)$$

where  $n_e$  is the electron number density of the WA gas. We assume that the electron number densities of the WAs gas and the ACM follow the power-law distributions:

$$\begin{aligned} n_e &= n_{e,0} \left( \frac{r}{r_0} \right)^{-m}, \\ n_{\text{ACM}} &= n_{\text{ACM},0} \left( \frac{r}{r_0} \right)^{-k}, \end{aligned} \quad (5)$$

where  $r_0$  is the launching radius of the WA cloud,  $n_{e,0}$  is the number density of WA cloud at  $r_0$  and  $n_{\text{ACM},0}$

is the number density of the ACM at  $r_0$ . Therefore, combining Equations 4–5, we can obtain a correlation between  $\xi$  and  $v_{\text{out}}$ :

$$v_{\text{out}} = \left[ \frac{L_{\text{ion}}^{\frac{m-k}{m-2}}}{2\pi m_p c} \cdot \frac{n_{e,0}^{\frac{k-2}{m-2}}}{n_{\text{ACM},0}} \cdot r_0^{\frac{2(k-m)}{m-2}} \right]^{1/2} \xi^{\frac{k-2}{2(m-2)}} \quad (6)$$

### 3. DATA AND FITTING

In order to describe the correlation between  $v_{\text{out}}$  and  $\xi$  of WAs for the observational data in individual AGN (see Equation 6), high-resolution X-ray spectra and at least four WA components are required. Finally, we collect the parameters of WAs from the previously published papers for the following six Seyfert 1 galaxies (see Table 1):

- NGC 3227: Wang et al. (2022) found four WA components using the *XMM-Newton* spectra data.
- NGC 3783: Fu et al. (2017) found five WA components through fitting the *XMM-Newton* spectra, while Mao et al. (2019) found nine WA components using both the *XMM-Newton* and *Chandra* data.

**Table 2.** Best-fit parameters of  $\log[v_{\text{out}} (\text{km s}^{-1})] = a \times \log[\xi (\text{erg cm s}^{-1})] + b$  using LINMIX, ODR, and BCES methods, and index  $k$  of the density profile of the ACM.

Sources	Data	$\log[v_{\text{out}} (\text{km s}^{-1})] = a \times \log[\xi (\text{erg cm s}^{-1})] + b$				$k = 2a(m - 2) + 2$ $k (m = 1.42)^\dagger$
		Parameter	Fitting method			
			LINMIX	ODR	BCES	
Individual source						
NGC 3227	W22	$a$	$\lesssim 0.24$	$0.25 \pm 0.11^\star$	$0.35 \pm 0.10$	$1.71 \pm 0.13$
		$b$	$\lesssim 2.15$	$2.16 \pm 0.29$	$1.93 \pm 0.32$	
NGC 4051	L11	$a$	$0.19 \pm 0.06^\star$	$0.20 \pm 0.10$	$0.03 \pm 0.09$	$1.78 \pm 0.07$
		$b$	$2.36 \pm 0.13$	$2.35 \pm 0.20$	$2.79 \pm 0.23$	
NGC 4593	E13	$a$	$\lesssim 0.18$	$0.27 \pm 0.24$	$0.18 \pm 0.10^\star$	$1.79 \pm 0.11$
		$b$	$\lesssim 2.06$	$2.09 \pm 0.58$	$2.33 \pm 0.19$	
NGC 5548	E16	$a$	$0.10 \pm 0.09^\star$	$0.13 \pm 0.18$	$0.24 \pm 0.12$	$1.88 \pm 0.10$
		$b$	$2.62 \pm 0.19$	$2.54 \pm 0.42$	$2.34 \pm 0.34$	
NGC 3783	F17	$a$	$-0.13 \pm 0.03^\star$	$-0.16 \pm 0.12$	$-0.31 \pm 0.10$	$2.15 \pm 0.03$
		$b$	$3.02 \pm 0.06$	$3.04 \pm 0.11$	$3.17 \pm 0.12$	
	MJ19	$a$	$-0.08 \pm 0.03^\star$	$-0.10 \pm 0.07$	$-0.08 \pm 0.09$	$2.09 \pm 0.03$
		$b$	$3.05 \pm 0.06$	$3.09 \pm 0.08$	$3.04 \pm 0.21$	
NGC 7469	MM18	$a$	$\lesssim 0.64$	$-0.06 \pm 0.20$	$0.06 \pm 0.19$	...
		$b$	$\lesssim -0.56$	$2.88 \pm 0.55$	$2.54 \pm 0.47$	
Total						
NGC 3227 & 4051 & 4593 & 5548	W22 & L11 & E13 & E16	$a$	$0.19 \pm 0.02^\star$	$0.20 \pm 0.03$	$0.26 \pm 0.06$	$1.78 \pm 0.02$
		$b$	$2.37 \pm 0.05$	$2.36 \pm 0.07$	$2.25 \pm 0.16$	

NOTE—  $^\dagger m = 1.42$  is obtained for a sample of 35 Seyfert 1 galaxies from Tombesi et al. (2013) using the absorption measure distribution. The fitting results followed by “ $\star$ ” are used to calculate the index  $k$  and are plotted in Figure 1. The observational data are from the previously published papers: Wang et al. (2022) (W22), Fu et al. (2017) (F17), Mao et al. (2019) (MJ19), Lobban et al. (2011) (L11), Ebrero et al. (2013) (E13), Ebrero et al. (2016) (E16), and Mehdipour et al. (2018) (MM18). The data of NGC 3227, NGC 4051, NGC 4593, and NGC 5548 are also fitted together as a reference (see “NGC 3227 & 4051 & 4593 & 5548” in the “Total”).

- NGC 4051: Lobban et al. (2011) found five WA components using the *Chandra* spectral data.
- NGC 4593: Ebrero et al. (2013) found four WA components through fitting the spectra of *XMM-Newton* and *Chandra*.
- NGC 5548: Ebrero et al. (2016) found six WA components through fitting the spectra of *XMM-Newton* and *Chandra* (H02 data in Ebrero et al. 2016).
- NGC 7469: Mehdipour et al. (2018) found four WA components through fitting the spectra of *Chandra*.

Then we fit the correlation between  $\xi$  and  $v_{\text{out}}$  in each source using the following linear model:

$$\log[v_{\text{out}} (\text{km s}^{-1})] = a \times \log[\xi (\text{erg cm s}^{-1})] + b, \quad (7)$$

where  $a$  corresponds to the theoretical index  $(k - 2)/[2(m - 2)]$  in Equation 6, i.e.,  $a = (k - 2)/[2(m - 2)]$ . Therefore, the index of the density profile of the ACM can be calculated by

$$k = 2a(m - 2) + 2. \quad (8)$$

We mainly use LINMIX<sup>1</sup> method (Kelly 2007) to fit the observational data. The LINMIX method performs the linear regression based on a Bayesian approach, which runs a Markov-chain-Monte-Carlo algorithm to calculate the posterior distribution and can account for measurement errors on both variables in the fit. However, for NGC 3227 and NGC 4593, this method can only give an upper limit for the parameters (see Table 2). Therefore, we also use the following two methods as supplements: Orthogonal Distance Regression<sup>2</sup> (ODR; Boggs et al. 1989), and bivariate correlated errors and intrinsic scatter<sup>3</sup> (BCES; Akritas & Bershady 1996; Nemmen et al. 2012). Both of these two methods can also deal with measurements errors on both variables. The BCES method is a weighted least squares estimator, and the ODR method uses the least squares method to minimize the weighed orthogonal distance from the data to

<sup>1</sup> <https://linmix.readthedocs.io/en/latest/src/linmix.html>

<sup>2</sup> <https://docs.scipy.org/doc/scipy/reference/odr.html>

<sup>3</sup> <https://github.com/rsnemmen/BCES>

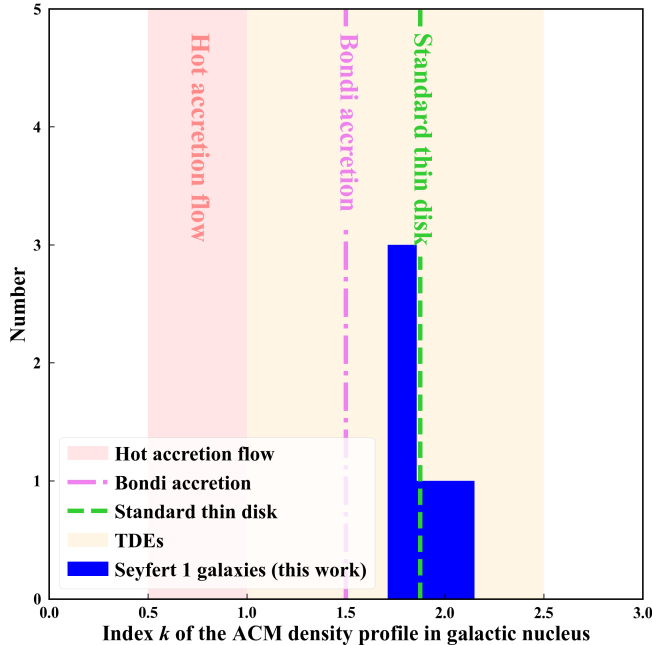


**Figure 2.** The distribution of the ACM density profile index  $k$  for the five Seyfert 1 galaxies (NGC 3227, NGC 4051, NGC 4593, NGC 5548, and NGC 3783) in this work (blue histogram). The green dashed line represents the predicted index by the standard thin disk model (Frank et al. 2002). The purple dash-dotted line represents the predicted index by the Bondi accretion model (Frank et al. 2002). The red region represents the predicted range of the index by the hot accretion flow simulations (Yuan et al. 2012). The yellow region represents the observational range of the index in TDEs (Alexander et al. 2020).

the fitted curve. The LINMIX method can provide a consistent fitting result to at least one of the other two methods (see Table 2).

#### 4. RESULTS

As Figure 1 shows, there is a positive correlation between  $v_{\text{out}}$  and  $\xi$  for NGC 3227, NGC 4051, NGC 4593, and NGC 5548 (The coefficient  $a$  of Equation 7 ranges from 0.10 to 0.25; also see Table 2), while NGC 3783 shows a negative correlation. For NGC 3783,  $a$  is  $-0.13 \pm 0.03$  for the data from Fu et al. (2017), and is  $-0.08 \pm 0.03$  for the data from Mao et al. (2019). However, the error bar of coefficient  $a$  is large, so we fit the data of NGC 3227, NGC 4051, NGC 4593, and NGC 5548 together as a reference, resulting in  $a = 0.19 \pm 0.02$ . The fitting result in individual source is consistent with the total fitting result in the sample. As mentioned in Section 1, the power-law indexes  $a$  for these Seyfert 1 galaxies are smaller than the predicted values by the theories: 0.5 for the radiatively driven outflowing mechanism, and larger than 0.5 for the MHD

driven outflowing mechanism. The  $v_{\text{out}} - \xi$  relation of NGC 7469 cannot be constrained, so its ACM density profile will not be discussed further (see Table 2), and its observational data are shown in Figure 1 as a reference.

The number density distribution of WAs can be estimated by the absorption measure distribution (Holzner et al. 2007; Behar 2009). Tombesi et al. (2013) estimated that  $m = 1.42$  for WAs in a sample of 35 Seyfert 1 galaxies. Combining Equation 8 and  $m = 1.42$  (Tombesi et al. 2013), the density profiles of the ACM in these Seyfert 1 galaxies are estimated to be between  $n \propto r^{-1.7}$  and  $n \propto r^{-2.15}$  (see Table 2) from 0.01 pc to pc scales, or even larger scales (the distance range of WAs). Both Tombesi et al. (2013) and Laha et al. (2014) investigated the correlation between  $v_{\text{out}}$  and  $\xi$  for WAs in a large AGN sample, which obtained  $a = 0.31$  and  $a = 0.12$ , respectively. Therefore, index of  $k$  is 1.64 and 1.82 for Tombesi et al. (2013) and Laha et al. (2014), respectively. Our results are similar to those in AGN samples. The density profile indexes  $k$  of the ACM in the five Seyfert 1 galaxies of our sample (NGC 3227, NGC 3783, NGC 4051, NGC 4593, and NGC 5548) are within the range of  $k$  for the ACM in TDEs (between  $-1$  and  $-2.5$ ; Alexander et al. 2020) (see Figure 2).

The density profile of the ACM within the Bondi radius might be connected to the accretion models. The Bondi radius can be expressed by  $r_B = 2GM_{\text{BH}}/c_{s,\infty}^2$ , where  $M_{\text{BH}}$  is the SMBH mass and  $c_{s,\infty}$  is the sound speed at infinity (Bondi 1952). For simplicity, we assume that the sound speeds at infinity of our sample are similar to that of M87 ( $r_B = 0.11$ – $0.22$  kpc with  $M_{\text{BH}} = 3.5 \times 10^9 M_{\odot}$ ; Russell et al. 2015) and Sgr A\* ( $r_B = 0.4$  pc with  $M_{\text{BH}} = 4 \times 10^6 M_{\odot}$ ; Li et al. 2015). Thus, according to the average  $M_{\text{BH}}$  of our sample ( $\sim 10^7 M_{\odot}$ ; Bentz & Katz 2015), the Bondi radii of our sample might be between 0.5 pc and 1 pc. Warm absorbers can exist from the scale within the Bondi radius (e.g., Ebrero et al. 2016; Wang et al. 2022) to the kpc scale (Laha et al. 2021). Although the large scale might not be associated with the accretion flow, given that most of the WAs in our sample might be located within or around the Bondi radius (e.g., Ebrero et al. 2016; Wang et al. 2022), we can briefly compare the density profiles between the ACM and the accretion flow here. The indexes  $k$  of the five Seyfert 1 galaxies are larger than the predicted value by the spherically symmetrical Bondi accretion model ( $-1.5$ ; Frank et al. 2002) and the simulated results of the hot accretion flow (between  $-0.5$  and  $-1.0$ ; Yuan et al. 2012), but relatively consistent with the prediction by the standard thin disk model ( $-15/8$ ; Frank et al. 2002) (see Figure 2).

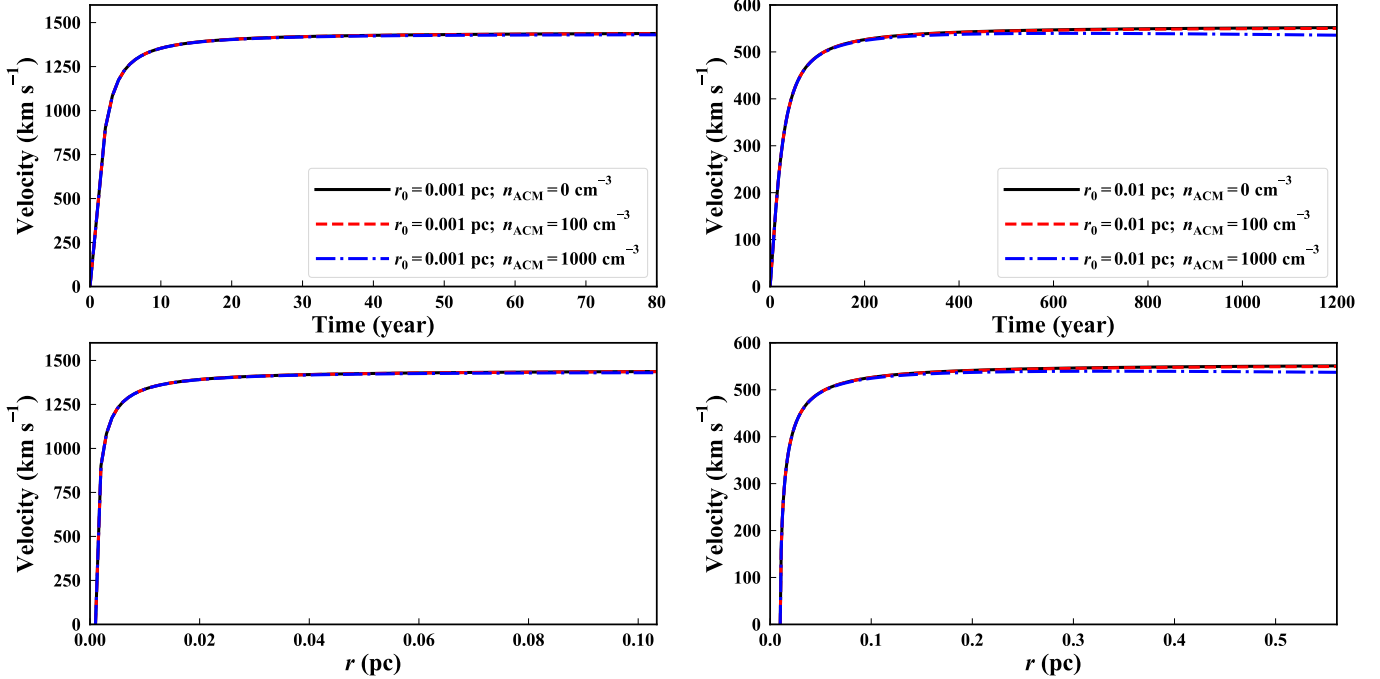


**Figure 3.** Estimating the acceleration timescale of WA outflows. The left two panels show the case of the launching radius ( $r_0$ ) of 0.001 pc and the right two panels show the case of the launching radius of 0.01 pc. The black solid, red dashed and blue dash-dotted lines represent the calculation of the ACM number density ( $n_{\text{ACM}}$ ) of  $0 \text{ cm}^{-3}$ ,  $100 \text{ cm}^{-3}$ , and  $1000 \text{ cm}^{-3}$ , respectively. It is obvious that the acceleration timescale is much shorter than the lifetime of WA.

## 5. DISCUSSIONS

### 5.1. Acceleration timescale required before equilibrium

To verify whether the assumption about the pressure equilibrium is feasible, we firstly estimate the acceleration timescale before reaching equilibrium of WA outflows. Under the action of the radiation pressure and drag pressure, the motion equation of the WA clouds is

$$\frac{v dv}{dr} = \frac{f_L L_{\text{ion}}}{4\pi c N_{\text{H}} m_{\text{p}} r^2} - \frac{C_{\text{D}} n_{\text{ACM}}}{2N_{\text{H}}} v^2, \quad (9)$$

where  $f_L$  is the fraction of the ionizing luminosity being absorbed or scattered by the WA cloud, which is about 2% according to Grafton-Waters et al. (2020) and Wang et al. (2022) and  $m_{\text{p}}$  is the mass of proton. The average ionizing luminosity of the sources in our sample is  $5 \times 10^{43} \text{ erg s}^{-1}$ . We simply set a constant column density to be  $N_{\text{H}} = 10^{22.5} \text{ cm}^{-2}$ , which is the maximum  $N_{\text{H}}$  for WAs obtained in AGN samples (Tombesi et al. 2013; Laha et al. 2014). As shown in Figure 3, we calculate the acceleration timescale for the launching radii  $r_0$  of 0.001 pc and 0.01 pc, with  $n_{\text{ACM}}$  being  $0 \text{ cm}^{-3}$ ,  $100 \text{ cm}^{-3}$ , and  $1000 \text{ cm}^{-3}$ . For the WA component that is close to the SMBH, the typical acceleration distance might be about 0.01 pc and the typical acceleration timescale might be about 10 years (see the left two panels of Figure 3), while the existence distance of this WA component might be larger than 0.01 pc (Laha et al. 2021), which means that

its existence timescale might be longer than its acceleration timescale. For the WA component that is relatively farther, the typical acceleration distance might be about 0.05 pc and the typical acceleration timescale might be about 100 years (see the right two panels of Figure 3), while the existence distance of this WA component is larger than 0.05 pc (e.g., Ebrero et al. 2016; Wang et al. 2022), which indicates that its acceleration timescale might be shorter than the existence timescale. These imply that the lifetimes of WAs are much larger than the acceleration timescales. These results indicate that WAs can stay in an equilibrium state during the most periods of their life.

### 5.2. Imbalance caused by AGN variabilities

The AGN variabilities can break the equilibrium state of WAs. Assuming the central luminosity changes from  $L$  to  $L'$  with  $L' = (1+f)L$ , the radiation pressure acting on each component of WAs along the line of sight will become  $P'_{\text{rad}} = (1+f)P_{\text{rad}}$  one by one. According to Equations. 1 and 2, then we can easily find that  $P'_{\text{rad}} = (1+f)P_{\text{D}}$  for each component of WAs. This means that the variability only has an impact on the estimation for the coefficient of Eq. 6 rather than the index. That is to say, even if the AGN variabilities are considered, the estimation for the index of the ACM density profile will not be affected.

## 6. SUMMARY

In this work, we propose a novel method to measure the ACM density profile by the equilibrium between the radiation pressure on the WA outflows and the drag pressure from the ACM for the following six Seyfert 1 galaxies: NGC 3227, NGC 3783, NGC 4051, NGC 4593, NGC 5548, and NGC 7469.

We study the correlation between outflow velocity and ionization parameter of the WAs in five Seyfert 1 galaxies of our sample (NGC 3227, NGC 3783, NGC 4051, NGC 4593, and NGC 5548). According to the fitting results of the  $v_{\text{out}} - \xi$  relation, we infer that the density profile of the ACM is between  $n \propto r^{-1.7}$  and  $n \propto r^{-2.15}$  from 0.01 pc to pc scales in these five AGNs. The indexes of the ACM density profiles in these five Seyfert galaxies are within the range of the indexes in TDEs. Our results indicate that the ACM density profile in Seyfert 1 galaxies is steeper than the prediction by the spherically symmetric Bondi accretion model and the

simulation results of the hot accretion flow, but more in line with the prediction by the standard thin disk model.

1 We thank the referee for constructive comments that im-  
 2 proved this paper. Y.J.W. acknowledges support from  
 3 the start-up research fund of School of Astronomy and  
 4 Space Science of Nanjing University. Y.J.W. and Y.Q.X.  
 5 acknowledge support from NSFC-12025303, 11890693,  
 6 the CAS Frontier Science Key Research Program  
 7 (QYZDJ-SSW-SLH006), and the K.C. Wong Education  
 8 Foundation. Z.-C. H. is supported by NSFC-11903031,  
 9 12192220, 12192221 and USTC Research Funds of the  
 10 Double First-Class Initiative YD 3440002001. This re-  
 11 search has made use of the NASA/IPAC Extragalactic  
 12 Database (NED), which is funded by the National Aero-  
 13 nautics and Space Administration and operated by the  
 14 California Institute of Technology.

## REFERENCES

- Akritas, M. G., & Bershadsky, M. A. 1996, *ApJ*, 470, 706, doi: [10.1086/177901](https://doi.org/10.1086/177901)
- Alexander, K. D., Berger, E., Guillochon, J., Zauderer, B. A., & Williams, P. K. G. 2016, *ApJL*, 819, L25, doi: [10.3847/2041-8205/819/2/L25](https://doi.org/10.3847/2041-8205/819/2/L25)
- Alexander, K. D., van Velzen, S., Horesh, A., & Zauderer, B. A. 2020, *SSRv*, 216, 81, doi: [10.1007/s11214-020-00702-w](https://doi.org/10.1007/s11214-020-00702-w)
- Anderson, M. M., Mooley, K. P., Hallinan, G., et al. 2020, *ApJ*, 903, 116, doi: [10.3847/1538-4357/abb94b](https://doi.org/10.3847/1538-4357/abb94b)
- Batchelor, G. K. 2000, *An Introduction to Fluid Dynamics*
- Begelman, M. C., McKee, C. F., & Shields, G. A. 1983, *ApJ*, 271, 70, doi: [10.1086/161178](https://doi.org/10.1086/161178)
- Behar, E. 2009, *ApJ*, 703, 1346, doi: [10.1088/0004-637X/703/2/1346](https://doi.org/10.1088/0004-637X/703/2/1346)
- Bentz, M. C., & Katz, S. 2015, *PASP*, 127, 67, doi: [10.1086/679601](https://doi.org/10.1086/679601)
- Blandford, R. D., & Payne, D. G. 1982, *MNRAS*, 199, 883, doi: [10.1093/mnras/199.4.883](https://doi.org/10.1093/mnras/199.4.883)
- Blustin, A. J., Page, M. J., Fuerst, S. V., Branduardi-Raymont, G., & Ashton, C. E. 2005, *A&A*, 431, 111, doi: [10.1051/0004-6361:20041775](https://doi.org/10.1051/0004-6361:20041775)
- Boggs, P. T., Donaldson, J. R., Byrd, R. h., & Schnabel, R. B. 1989, *ACM Trans. Math. Softw.*, 15, 348364, doi: [10.1145/76909.76913](https://doi.org/10.1145/76909.76913)
- Bondi, H. 1952, *MNRAS*, 112, 195, doi: [10.1093/mnras/112.2.195](https://doi.org/10.1093/mnras/112.2.195)
- Chen, Z., He, Z., Ho, L. C., et al. 2022, *Nature Astronomy*, doi: [10.1038/s41550-021-01561-3](https://doi.org/10.1038/s41550-021-01561-3)
- Ebrero, J., Kaastra, J. S., Kriss, G. A., de Vries, C. P., & Costantini, E. 2013, *MNRAS*, 435, 3028, doi: [10.1093/mnras/stt1497](https://doi.org/10.1093/mnras/stt1497)
- Ebrero, J., Kaastra, J. S., Kriss, G. A., et al. 2016, *A&A*, 587, A129, doi: [10.1051/0004-6361/201527808](https://doi.org/10.1051/0004-6361/201527808)
- Eftekhari, T., Berger, E., Zauderer, B. A., Margutti, R., & Alexander, K. D. 2018, *ApJ*, 854, 86, doi: [10.3847/1538-4357/aaa8e0](https://doi.org/10.3847/1538-4357/aaa8e0)
- Elvis, M. 2000, *ApJ*, 545, 63, doi: [10.1086/317778](https://doi.org/10.1086/317778)
- Frank, J., King, A., & Raine, D. J. 2002, *Accretion Power in Astrophysics: Third Edition*
- Fu, X.-D., Zhang, S.-N., Sun, W., Niu, S., & Ji, L. 2017, *Research in Astronomy and Astrophysics*, 17, 095, doi: [10.1088/1674-4527/17/9/95](https://doi.org/10.1088/1674-4527/17/9/95)
- Fukumura, K., Kazanas, D., Contopoulos, I., & Behar, E. 2010, *ApJ*, 715, 636, doi: [10.1088/0004-637X/715/1/636](https://doi.org/10.1088/0004-637X/715/1/636)
- Gezari, S. 2021, *Annual Review of Astronomy and Astrophysics*, 59, null, doi: [10.1146/annurev-astro-111720-030029](https://doi.org/10.1146/annurev-astro-111720-030029)
- Gillessen, S., Plewa, P. M., Widmann, F., et al. 2019, *ApJ*, 871, 126, doi: [10.3847/1538-4357/aaf4f8](https://doi.org/10.3847/1538-4357/aaf4f8)
- Gofford, J., Reeves, J. N., McLaughlin, D. E., et al. 2015, *MNRAS*, 451, 4169, doi: [10.1093/mnras/stv1207](https://doi.org/10.1093/mnras/stv1207)
- Grafton-Waters, S., Branduardi-Raymont, G., Mehdipour, M., et al. 2020, *A&A*, 633, A62, doi: [10.1051/0004-6361/201935815](https://doi.org/10.1051/0004-6361/201935815)
- He, Z., Wang, T., Liu, G., et al. 2019, *Nature Astronomy*, 3, 265, doi: [10.1038/s41550-018-0669-8](https://doi.org/10.1038/s41550-018-0669-8)

- Holczer, T., Behar, E., & Kaspi, S. 2007, *ApJ*, 663, 799, doi: [10.1086/518416](https://doi.org/10.1086/518416)
- Kaasra, J. S., Mewe, R., Liedahl, D. A., Komossa, S., & Brinkman, A. C. 2000, *A&A*, 354, L83. <https://arxiv.org/abs/astro-ph/0002345>
- Kelly, B. C. 2007, *ApJ*, 665, 1489, doi: [10.1086/519947](https://doi.org/10.1086/519947)
- King, A., & Pounds, K. 2015, *ARA&A*, 53, 115, doi: [10.1146/annurev-astro-082214-122316](https://doi.org/10.1146/annurev-astro-082214-122316)
- Laha, S., Guainazzi, M., Dewangan, G. C., Chakravorty, S., & Kembhavi, A. K. 2014, *MNRAS*, 441, 2613, doi: [10.1093/mnras/stu669](https://doi.org/10.1093/mnras/stu669)
- Laha, S., Reynolds, C. S., Reeves, J., et al. 2021, *Nature Astronomy*, 5, 13, doi: [10.1038/s41550-020-01255-2](https://doi.org/10.1038/s41550-020-01255-2)
- Li, Y.-P., Yuan, F., & Wang, Q. D. 2015, *ApJ*, 798, 22, doi: [10.1088/0004-637X/798/1/22](https://doi.org/10.1088/0004-637X/798/1/22)
- Lobban, A. P., Reeves, J. N., Miller, L., et al. 2011, *MNRAS*, 414, 1965, doi: [10.1111/j.1365-2966.2011.18513.x](https://doi.org/10.1111/j.1365-2966.2011.18513.x)
- Mao, J., Mehdipour, M., Kaasra, J. S., et al. 2019, *A&A*, 621, A99, doi: [10.1051/0004-6361/201833191](https://doi.org/10.1051/0004-6361/201833191)
- Mehdipour, M., Kaasra, J. S., Costantini, E., et al. 2018, *A&A*, 615, A72, doi: [10.1051/0004-6361/201832604](https://doi.org/10.1051/0004-6361/201832604)
- Miller, M. J., & Bregman, J. N. 2015, *ApJ*, 800, 14, doi: [10.1088/0004-637X/800/1/14](https://doi.org/10.1088/0004-637X/800/1/14)
- Mizumoto, M., Done, C., Tomaru, R., & Edwards, I. 2019, *MNRAS*, 489, 1152, doi: [10.1093/mnras/stz2225](https://doi.org/10.1093/mnras/stz2225)
- Mo, H., van den Bosch, F. C., & White, S. 2010, *Galaxy Formation and Evolution*
- Narayan, R., & Yi, I. 1994, *ApJL*, 428, L13, doi: [10.1086/187381](https://doi.org/10.1086/187381)
- Nemmen, R. S., Georganopoulos, M., Guiriec, S., et al. 2012, *Science*, 338, 1445, doi: [10.1126/science.1227416](https://doi.org/10.1126/science.1227416)
- Proga, D., & Kallman, T. R. 2004, *ApJ*, 616, 688, doi: [10.1086/425117](https://doi.org/10.1086/425117)
- Reynolds, C. S. 1997, *MNRAS*, 286, 513, doi: [10.1093/mnras/286.3.513](https://doi.org/10.1093/mnras/286.3.513)
- Reynolds, C. S., & Fabian, A. C. 1995, *MNRAS*, 273, 1167, doi: [10.1093/mnras/273.4.1167](https://doi.org/10.1093/mnras/273.4.1167)
- Russell, H. R., Fabian, A. C., McNamara, B. R., & Broderick, A. E. 2015, *MNRAS*, 451, 588, doi: [10.1093/mnras/stv954](https://doi.org/10.1093/mnras/stv954)
- Shakura, N. I., & Sunyaev, R. A. 1973, *A&A*, 500, 33
- Silva, C. V., Costantini, E., Giustini, M., et al. 2018, *MNRAS*, 480, 2334, doi: [10.1093/mnras/sty1938](https://doi.org/10.1093/mnras/sty1938)
- Tarter, C. B., Tucker, W. H., & Salpeter, E. E. 1969, *ApJ*, 156, 943, doi: [10.1086/150026](https://doi.org/10.1086/150026)
- Tombesi, F., Cappi, M., Reeves, J. N., et al. 2013, *MNRAS*, 430, 1102, doi: [10.1093/mnras/sts692](https://doi.org/10.1093/mnras/sts692)
- Wang, Y., Kaasra, J., Mehdipour, M., et al. 2022, *A&A*, 657, A77, doi: [10.1051/0004-6361/202141599](https://doi.org/10.1051/0004-6361/202141599)
- Wong, K.-W., Irwin, J. A., Yukita, M., et al. 2011, *ApJL*, 736, L23, doi: [10.1088/2041-8205/736/1/L23](https://doi.org/10.1088/2041-8205/736/1/L23)
- Yuan, F., & Narayan, R. 2014, *ARA&A*, 52, 529, doi: [10.1146/annurev-astro-082812-141003](https://doi.org/10.1146/annurev-astro-082812-141003)
- Yuan, F., Wu, M., & Bu, D. 2012, *ApJ*, 761, 129, doi: [10.1088/0004-637X/761/2/129](https://doi.org/10.1088/0004-637X/761/2/129)